Supporting Information:

Ultrafast Charge Carrier Recombination and Trapping in Hematite Photoanodes under Applied Bias

Stephanie R Pendlebury,[†] Xiuli Wang,[†] Florian le Formal,[†] Maurin Cornuz,[‡] Andreas Kafizas,[†] S. David Tilley,[‡] Michael Grätzel,[‡] James R Durrant[†]

[†]Department of Chemistry, Imperial College London, South Kensington Campus, London, SW7 2AZ, United Kingdom

[‡]Institut des Sciences et Ingénierie Chimiques, Ecole Polytechnique Fédérale de Lausanne, Laboratory of Photonics and Interfaces, Station 6, CH-1015 Lausanne, Switzerland

Experimental

Hematite and Titania photoanodes:

Si-doped hematite (α-Fe_2O_3) photoanodes with dendritic nanostructure, deposited on FTO-glass by APCVD (atmospheric pressure chemical vapor deposition), were employed for the majority of the studies reported herein and in the main paper. Full synthetic details and characterisation of these photoanodes have previously been reported in detail in the literature.[1-3] Nanostructured APCVD "undoped" (with no Si-dopant) hematite (on FTO) was also investigated.[1] UV-vis spectra are shown below.

Nanocrystalline anatase titania (n-TiO_2) porous photoanodes consist of ~30 nm diameter particles deposited on FTO glass by the doctor-blading method,[4] to a thickness of approx. 3.7 µm. Dense anatase TiO_2 was grown on quartz substrate by APCVD from the reaction of titanium tetrachloride and ethyl acetate at 500 °C, where full synthetic details have previously been reported.[5] UV-vis spectra are shown below.

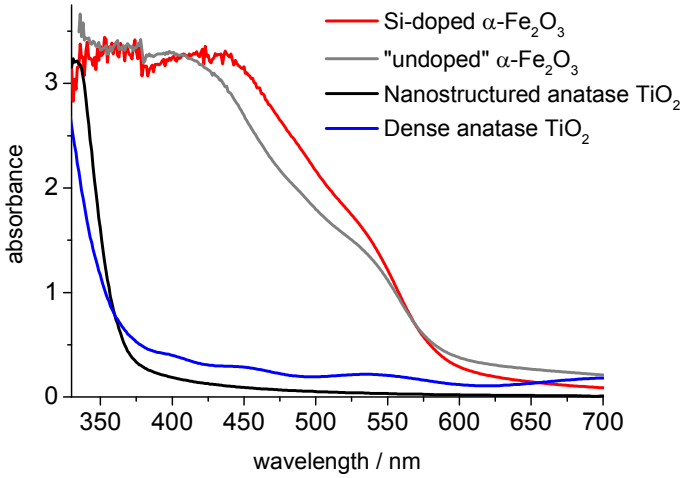

Fig S1: UV-visible absorbance spectra of the hematite and anatase TiO_2 samples.

The UV-vis spectrum of hematite changes with applied electrical bias; such spectroelectrochemical studies by our group have previously been reported in detail.[6,7]

fs-Transient Absorption Spectroscopy (TAS):

Transient absorption spectra were collected on fs-ns timescales using a regeneratively amplified Ti:sapphire laser system (Solstice, Spectra-Physics) and Helios spectrometers (Ultrafast Systems). The Solstice laser system generates 800 nm, 92 fs width, 1 kHz pulses. The excitation (pump) pulse is generated from a fraction of the 800 nm beam via an OPA (TOPAS Prime, Spectra-Physics) and frequency-mixer (NirUVis, Light Conversion) to select the wavelength, 355 nm (for comparison to µs-s TAS). The pump beam diameter is approximately 1 mm at the sample. The intensity of the pump beam was modulated using neutral density filters, and was measured using a 500 µm diameter aperture and power meter (PD10-V2-ROHS, OPHIR Photonics). The probe pulse is delayed with respect to the excitation pulse by a motorised translational stage, which changes the path length of the probe beam. A visible or NIR white light continuum (WLC) is used as the probe, generated by attenuating and focussing a fraction of the 800 nm pulse onto one of two Ti:sapphire crystals of different thicknesses. In order to reduce noise, the WLC is split into two beams: one passes through the sample while the other is monitored by the reference spectrometer. The beams are focussed into two fibre-optic-coupled multichannel spectrometers (CMOS or InGaAs sensors for visible and NIR wavelengths, respectively). A synchronised chopper (500 Hz) is used to block alternate pump pulses; the absorbance change is calculated from adjacent pulses (pump blocked and unblocked). Difference spectra were typically averaged over 2 seconds for each time point recorded; each spectrum was collected several times then averaged. Spectra were corrected for chirp (group velocity dispersion) using Surface Xplorer software (Ultrafast Systems) by fitting the rise of the spectrum. Spectra were time-zero corrected such that t_0 occurs at the half-amplitude of the spectrum rise. Individual decay kinetics shown are averaged over ~10 nm. Due to fluctuations of the laser intensity over time during these measurements, normalized kinetics are compared.

µs-s Transient Absorption Spectroscopy (TAS):

The home-built transient absorption spectrometer employed for these studies has been described previously.[8] The third harmonic (355 nm, 200 µJ.cm^{-2}.pulse^{-1}, 0.33 Hz, "EE" front-side excitation) of a Nd:YAG laser (Big Sky Laser Technologies, Ultra CFR Nd:YAG laser system, 6 ns pulse width) is employed as the pump, while the probe beam is the monochromated output of a 100 W tungsten lamp (Bantham IL1). The laser light is transmitted to the sample via a liquid light guide. A number of long-pass filters and a band-pass filter (Comar Instruments) were placed between the sample and the detector, in order to attenuate the scattered laser light. The transmittance of photons through the sample is measured by a Si photodiode detector (Hamamatsu S3071). Collected data were filtered and amplified (Costronics amplifier), and were then recorded with an oscilloscope (Tektronics TDS 2012c) on the timescale of µs – ms, and with a DAQ card (National Instruments, NI USB-6211) on the timescale of ms–s. All data were acquired by home-programmed Labview software. Data shown are the average of 300-500 laser shots, with the laser scatter subtracted.

Photoelectrochemistry:

For measurements in a working PEC cell, a three-electrode configuration was employed using a home-made PEEK cell with quartz windows. A Pt-gauze counter electrode and Ag│AgCl│sat.KCl reference electrode (Metrohm) were used in 0.1 M NaOH electrolyte, pH 12.8. Electrolyte solutions were prepared from NaOH (Sigma-Alrich, reagent grade, as received) and MilliQ deionised water (Millipore Corp., 18.2MΩ.cm at 25 °C); the electrolyte was not degassed. For fs-TAS measurements of hematite in a 3-electrode PEC cell, the voltage was applied using a Keithley sourcemeter as a pseudo-potentiostat; for µs-TAS a Sycopel ministat was employed. The current was allowed to stabilise before TAS measurements were begun. Herein, the applied voltage is reported *versus* the reversible hydrogen electrode (RHE), calculated using $E_{RHE}=E°+E+0.059pH$, where $E°$ is the standard potential of the Ag│AgCl│sat.KCl reference (~0.21 V_{RHE} at 25 °C), and E is the potential *versus* Ag│AgCl│sat.KCl. The photoanode (working electrode) was illuminated in the EE (electrolyte-electrode or "front side") direction. Current/voltage curves were acquired using a Metrohm ministat, employing a 75 W Xe lamp (OBB) with two homogenisers and a KG3 filter (Thorlabs). A silicon diode and a 650nm shortpass filter (Edumnd optics) were used to adjust the light intensity such that the number of photons per square centimeter at <650 nm (approximately the absorption edge of hematite) reaching the sample was equivalent to that of AM 1.5.

Estimation of Space-Charge Layer Width

The width of the space-charge layer (depletion region, W) can be estimated:

$$W = \sqrt{\frac{(V-V_{FB})2\varepsilon\varepsilon_0}{eN_D}} \qquad (2)$$

where V is the applied voltage, ε_0 is the permittivity of free space, and e is the charge on an electron. For hematite, taking the relative permittivity ε = 80, flatband potential V_{FB} = 0.5 V_{RHE}, and the donor density N_D = 1.5x10^{20} cm^{-3}, this gives W = ~7 nm at 1.4 V_{RHE} for the APCVD Si-Fe_2O_3 photoanode.[2] It is noted that literature values for the relative permittivity of hematite vary from 12 to 120,[9] thus this value of W should be taken as a ballpark figure.

Given the short hole diffusion length of a few nanometers in hematite,[10-12] essentially all carriers generated outside the SCL will undergo rapid bulk recombination. The nanostructured APCVD α-Fe_2O_3 photoanodes employed in the studies reported in the main paper have a dendritic nanostructure, with large particles close to the FTO substrate and small nanoparticles at the surface.[2] Although the smallest particles may be completely depleted under strong anodic bias, a significant fraction of the photoanode will be in the bulk region.

Results

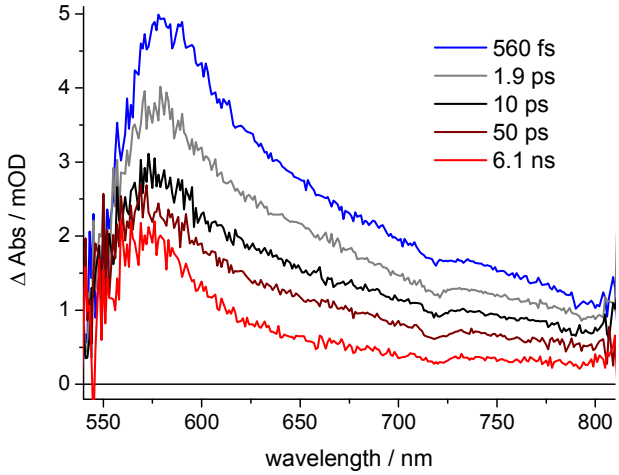

Fig S2: Transient absorption (TA) spectra of nanostructured Si-doped APCVD hematite in an inert atmosphere (N_2), under relatively low excitation density (355 nm, 500 Hz, 170 uJ.cm^{-2}.pulse^{-1}; ~2.75x10^{14} photons abs.cm^{-2}.pulse^{-1}). The legend indicated time after excitation by the pump pulse. There is a fast decay of the spectrum within the first 10 ps, which is not observed for TiO_2 (see below).

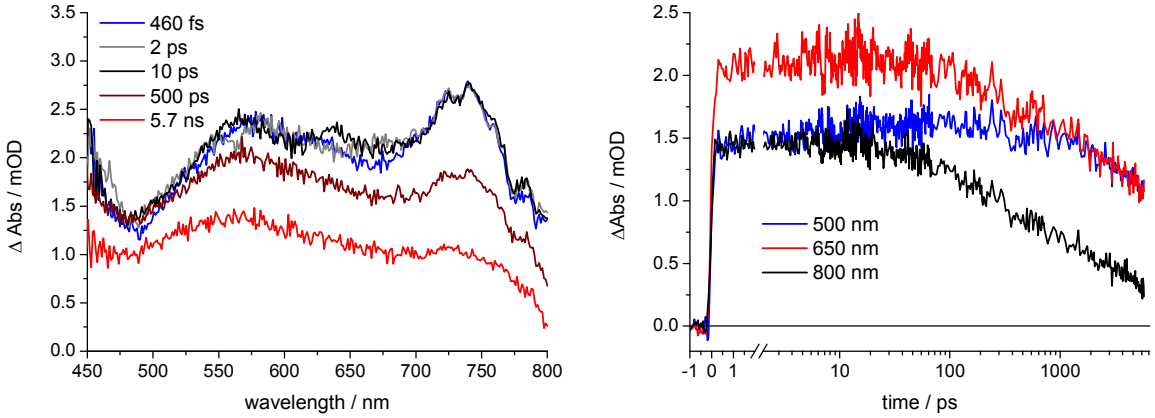

Fig S3: Transient absorption (TA) spectra (left) and kinetics (right; the legend indicates probe wavelength) of nanocrystalline anatase TiO_2 (n-TiO_2) in N_2 atmosphere, under relatively low excitation density (355 nm, 500 Hz, 320 µJ.cm^{-2}.pulse^{-1}, ~5.24x10^{14} photons abs.cm^{-2}.pulse^{-1}). The signal remains approximately constant until ~20 ps after excitation.

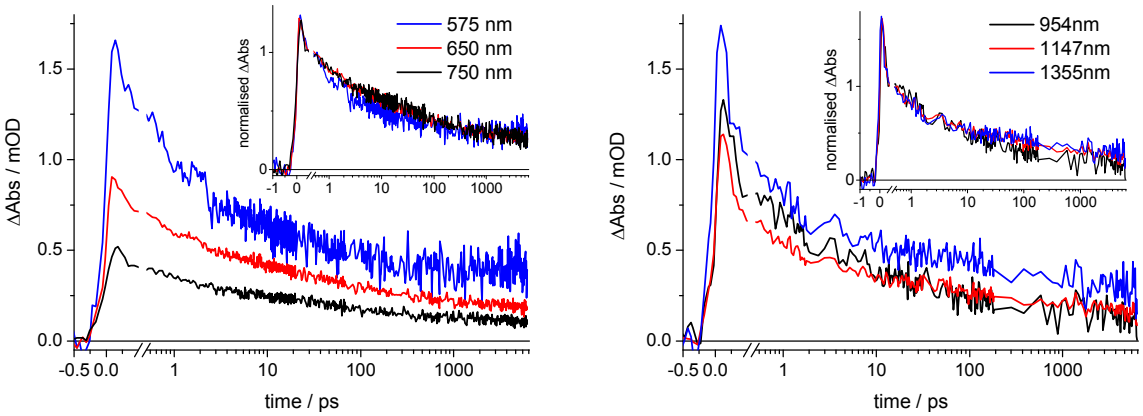

Fig S4: TA decay kinetics of Si-doped nanostructured APCVD hematite in a nitrogen atmosphere, under relatively weak excitation probed in the visible (left) and near-IR (right). The legend indicates probe wavelength. The signal exhibits a rapid decay which begins within the time resolution of the measurement (~200 fs). It is extremely unlikely that this initial decay phase is an artifact, since artifacts are symmetrical about $t = 0$,[13] and a fast initial transient optical decay is widely reported for hematite produced via several different synthetic routes.[14-20] Thus the TA signal is due to additional absorption by photogenerated charge carriers; the decay of this signal indicates the loss of charge carriers, either by recombination and/or trapping (relaxation).

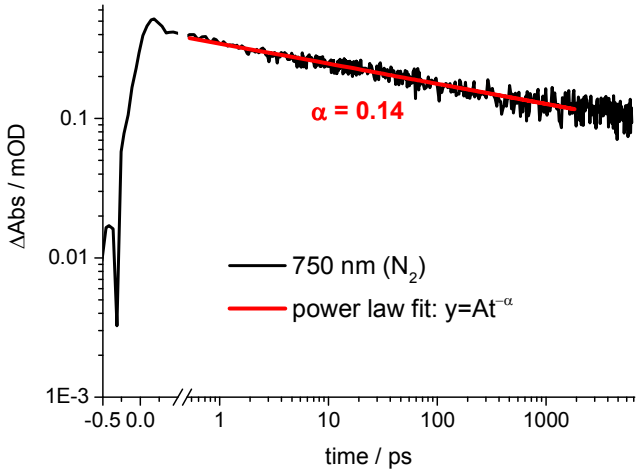

Fig S5: Example of a power law fit to the ultrafast transient absorption decay kinetics. Si-doped nanostructured APCVD hematite in a nitrogen atmosphere, probed at 750 nm (355 nm excitation, 42 μJ.cm^{-2}). TiO_2 decay kinetics shown in Figure 1B in the main paper also fit to a power law, with α=0.11 (fit between 5 ps–6 ns) for an excitation intensity of 82 μJ.cm^{-2}. Power law fits to the ultrafast TAS decays of Si-doped nanostructured hematite reported herein have $0.10<\alpha<0.35$.

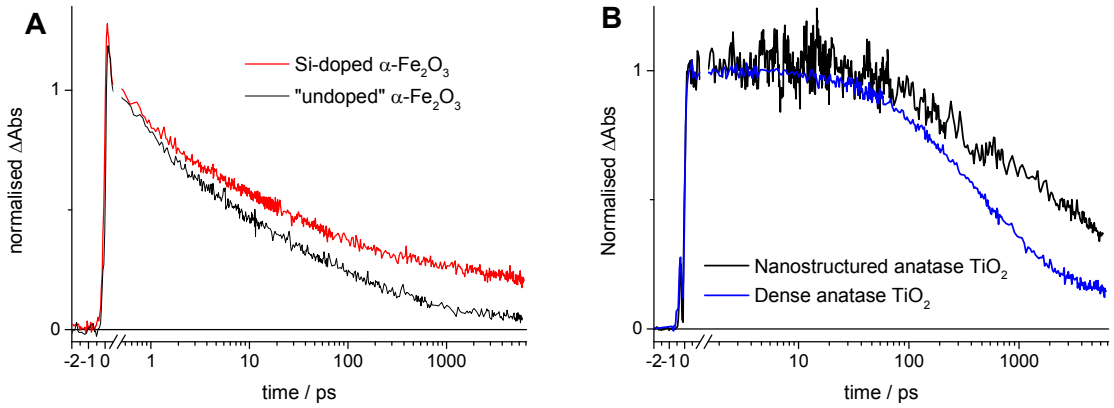

Fig S6: normalized TA decay kinetics of **(A)** Si-doped and "undoped" nanostructured APCVD hematite (in N_2, 355 nm excitation), probed at 750 nm; **(B)** nanocrystalline (nanostructured; ~30 nm particles, 3 μm thick film) and dense anatase (400 nm thick) (in N_2, 355 nm excitation). The two very different types of hematite both exhibit a fast decay, which begins within the time resolution of the measurements (*ca* 200 fs). Both nanostructured and dense (solid) anatase TiO_2 exhibit slower decay kinetics, with almost no recombination until >10 ps after excitation.

Even under strong anodic bias, a sizeable proportion of photogenerated carriers in hematite recombine within 6 ns, which represents a significant inherent limitation to the maximum possible solar energy conversion efficiency of hematite.

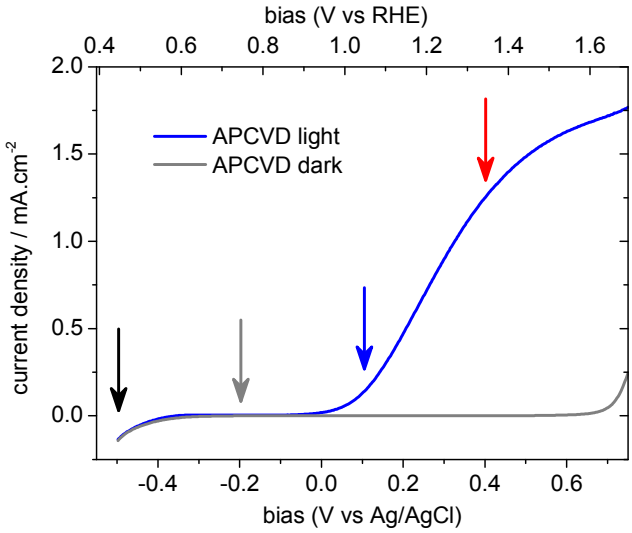

Fig S7: Current/voltage linear sweep voltammograms in the dark (grey line) and under approximately 1 Sun conditions (according to number of photons at wavelengths <600 nm; blue line; EE illumination) for nanostructured Si-doped APCVD hematite. The electrolyte was 0.1 M NaOH. Coloured arrows indicate the respective applied potentials employed in transient absorption studies.

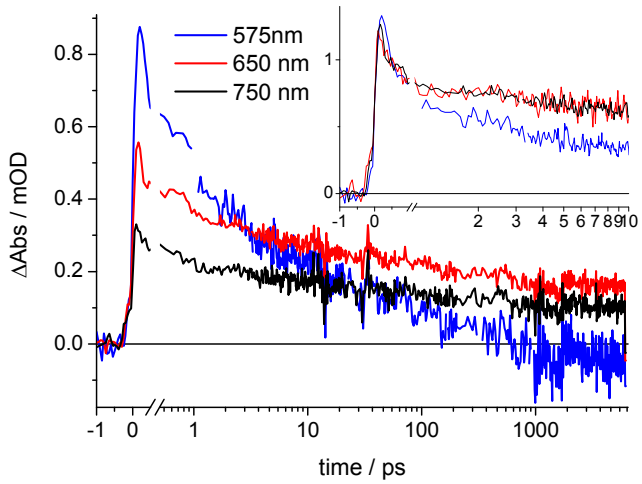

Fig S8: TA decay kinetics of Si-doped nanostructured APCVD hematite in 0.1 M NaOH (pH 12.8; no applied electrical bias), under relatively weak excitation (355 nm, 500 Hz, ~40 $\mu J.cm^{-2}.pulse^{-1}$). The legend indicates probe wavelength; the inset shows the first 10 ps of the normalized decay kinetics. The signal probed at ~575 nm decays faster than at other wavelengths, and bleaches after ~500 ps, due to oxidisation of trap states within the space-charge layer formed at the semiconductor-liquid junction. The signal probed at 650 and 750 nm exhibits a similar fast decay to that observed in N_2 (Figure 1 in the main paper and Figure S4).

References

(1) Kay, A.; Cesar, I.; Gratzel, M. *J. Am. Chem. Soc.* **2006**, *128*, 15714.
(2) Cesar, I.; Sivula, K.; Kay, A.; Zboril, R.; Gratzel, M. *J. Phys. Chem. C* **2009**, *113*, 772.
(3) Tilley, S. D.; Cornuz, M.; Sivula, K.; Gratzel, M. *Angew. Chem. Int. Ed.* **2010**, *49*, 6405.
(4) Gimeno, N.; Li, X.; Durrant, J. R.; Vilar, R. *Chem. Eur. J.* **2008**, *14*, 3006.
(5) Kafizas, A.; Carmalt, C. J.; Parkin, I. P. *Chem. Eur. J.* **2012**, *18*, 13048.
(6) Barroso, M.; Mesa, C. A.; Pendlebury, S. R.; Cowan, A. J.; Hisatomi, T.; Grätzel, M.; Klug, D. R.; Durrant, J. R. *PNAS* **2012**, *109*, 15640.
(7) Barroso, M.; Pendlebury, S. R.; Cowan, A. J.; Durrant, J. R. *Chem. Sci.* **2013**, *4*, 2724.
(8) Le Formal, F.; Pendlebury, S. R.; Cornuz, M.; Tilley, S. D.; Grätzel, M.; Durrant, J. R. *J. Am. Chem. Soc.* **2014**, *136*, 2564.
(9) Glasscock, J. A.; Barnes, P. R. F.; Plumb, I. C.; Bendavid, A.; Martin, P. J. *Thin Solid Films* **2008**, *516*, 1716.
(10) Kennedy, J. H.; Frese, K. W. *J. Electrochem. Soc.* **1978**, *125*, 709.
(11) Dare-Edwards, M. P.; Goodenough, J. B.; Hamnett, A.; Trevellick, P. R. *Journal of the Chemical Society-Faraday Transactions I* **1983**, *79*, 2027.
(12) Le Formal, F.; Sivula, K.; Grätzel, M. *The Journal of Physical Chemistry C* **2012**, *116*, 26707.
(13) Ruckebusch, C.; Sliwa, M.; Pernot, P.; de Juan, A.; Tauler, R. *J. Photochem. Photobiol. C* **2012**, *13*, 1.
(14) Cherepy, N. J.; Liston, D. B.; Lovejoy, J. A.; Deng, H.; Zhang, J. Z. *J. Phys. Chem. B* **1998**, *102*, 770.
(15) Nadtochenko, V. A.; Denisov, N. N.; Gak, V. Y.; Gostev, F. E.; Titov, A. A.; Sarkisov, O. M.; Nikandrov, V. V. *Russ. Chem. Bull.* **2002**, *51*, 457.
(16) Joly, A. G.; Williams, J. R.; Chambers, S. A.; Xiong, G.; Hess, W. P.; Laman, D. M. *J. Appl. Phys.* **2006**, *99*, 053521.

(17) Ling, Y.; Wang, G.; Wheeler, D. A.; Zhang, J. Z.; Li, Y. *Nano Lett.* **2011**, *11*, 2119.
(18) Huang, Z.; Lin, Y.; Xiang, X.; Rodríguez-Córdoba, W.; McDonald, K. J.; Hagen, K. S.; Choi, K.-S.; Brunschwig, B. S.; Musaev, D. G.; Hill, C. L.; Wang, D.; Lian, T. *Energy Environ. Sci.* **2012**, *5*, 8923.
(19) Shen, S.; Guo, P.; Wheeler, D. A.; Jiang, J.; Lindley, S. A.; Kronawitter, C. X.; Zhang, J. Z.; Guo, L.; Mao, S. S. *Nanoscale* **2013**, *5*, 9867.
(20) Fitzmorris, B. C.; Patete, J. M.; Smith, J.; Mascorro, X.; Adams, S.; Wong, S. S.; Zhang, J. Z. *ChemSusChem* **2013**, *6*, 1907.